Quantum Mechanical Single-Gold-Nanocluster Electroluminescent Light Source at Room Temperature

Jose I. Gonzalez,[1] Tae-Hee Lee,[1] Michael D. Barnes,[2] Yasuko Antoku,[1] and Robert M. Dickson[1,3,*]

[1]*School of Chemistry and Biochemistry, Georgia Institute of Technology, Atlanta, Georgia 30332-0400, USA*

[2]*Chemical Sciences Division, Oak Ridge National Laboratory, Oak Ridge, Tennessee, USA*

[3]*Center for Advanced Research in Optical Microscopy, Georgia Institute of Technology, Atlanta, Georgia 30332-0400, USA*

(Received 5 May 2004; published 27 September 2004; publisher error corrected 4 October 2004)

Electrically contacted gold-nanocluster arrays formed within electromigration-induced break junctions exhibit bright, field-dependent electroluminescence in the near infrared (650–800 nm). Intensity autocorrelation of spatially isolated individual nanocluster emission driven at high electrical frequency ($f_{ac} = \sim 200$ MHz) reveals antibunched electroluminescence at room temperature. These results demonstrate the single quantum nature of several-atom gold molecules and suggest their use as room-temperature electrically driven single-photon sources.

DOI: 10.1103/PhysRevLett.93.147402 PACS numbers: 78.60.Fi, 42.50.–p, 78.67.Bf, 85.60.Jb

The use of nonorthogonal bases with quantum mechanical sources is the cornerstone of many proposed ultrasecure encryption schemes [1–3]. Such methods ideally rely on the creation of highly polarized, wavelength-tunable pure single-photon states. While nonclassical *laser-induced* fluorescence has been observed for individual atoms [4–8], molecules [9,10], polymer nanostructures [11,12], color centers in diamond films [13,14], and semiconductor quantum dots [15–17], single molecule *electroluminescence* offers pronounced advantages by avoiding background, complexity, and cost resulting from high intensity laser excitation. Toward this goal, electrically driven nanoscale light sources have been demonstrated in carbon nanotube field-effect transistors [18], semiconductor nanowires [19], and semiconductor quantum dots at cryogenic temperature [20]. In this Letter, we demonstrate robust, nonclassical electroluminescence *at room temperature* from spatially isolated Au nanoclusters within easily fabricated dc-generated nanoscale break junctions. Behaving as single-quantum systems (analogous to multielectron artificial atoms) [21], these electrically contacted, spatially isolated gold nanoclusters exhibit clear photon antibunching in their strong, near-infrared electroluminescence. This result clearly establishes the viability of these species in a photonic quantum information processing context, and suggests a promising new direction in the field of nanoscale quantum optoelectronics.

As all materials must relax with a characteristic time constant before reexcitation, simultaneous emission of two or more photons is forbidden for spatially isolated single-quantum systems. Thus, single atoms [4–8], molecules [9,10], and even several-nm semiconductor quantum dots [15–17] have each been observed to emit no more than one photon at a time, independent of optical excitation intensity. The long-radiative lifetimes (> 1 ns) characteristic of these systems limit single-photon data rates but enable characterization with slower, high sensitivity detectors. Essential for quantum encryption, demonstration of pure single-photon emission from individual species is accomplished by measuring the intensity autocorrelation function, $g^{(2)}(\tau)$, in a Hanbury Brown and Twiss configuration [22] (Fig. 1). In such an arrangement, we measure the probability of detecting two individual photons as a function of arrival time *difference*, τ. Since simultaneous emission of two photons is forbidden for a single-quantum system, the intensity autocorrelation function approaches zero at zero delay, an effect known as *photon antibunching*. Observation of $g^{(2)}(0) \approx 0$ thus represents a definitive signature of sub-Poissonian light and is obtainable only from a true single-quantum mechanical source [23].

Recently, we created a new class of noble metal quantum dots that exhibit strong fluorescence in aqueous solution [21,24], as well as electroluminescence within deposited films [25,26]. Behaving as multielectron artificial atoms, these nanogold species should provide facile routes to producing strong single-photon emitters, even approaching telecommunication wavelengths. These sub-nm metal quantum dots have size-tunable emission throughout the visible and near infrared, with Au_{31}, for example, absorbing at 780 nm and emitting at 870 nm with high quantum yield [21]. Low density arrays of 18–22 atom Au nanoclusters can also be produced *in situ* during electromigration-induced nanoscale break junction formation [25], allowing facile electro-optical interrogation of individual strongly electroluminescent species. These moleculelike species exhibit clear dipolar radiation patterns [27] under optical and electrical excitation suggestive of individual quantum emitters (Fig. 2). While antibunched emission from electrically excited semiconductor quantum dots has been recently reported [20], this has only been possible in complicated nanofabricated devices at cryogenic temperatures due to the

shallow electron well and band structure of several-nanometer semiconductor quantum dots [28]. While a great advance, the nonclassical, long-radiative lifetime electroluminescence disappears rapidly with increasing temperature, precluding anything but cryogenic measurements. The several-atom size of our Au nanoclusters and their behavior as multielectron artificial atoms [21], dictates that the density of states is sufficiently low such that the energy level spacings are large compared to ambient thermal energies. Consequently, in contrast to much larger semiconductor quantum dots, these Au dots should easily continue to operate far into the near IR at room temperatures.

Strongly electroluminescent Au nanoclusters were produced within 25-nm thick Au films sputtered onto clean glass cover slips. Films were reduced to ~ 150 μm wide strips, and the ends were coated with small drops of silver paint for electrical contacts. The cover slip forms the bottom window of a microscope-mounted vacuum chamber ($< 10^{-5}$ torr) with the vacuum forcing electrical contact between spring-loaded electrodes and the silver paint. Application of 3 V, ~ 150 mA for ~ 10 s produces an electromigration-induced break junction near the center of the Au film, creating highly emissive Au nanoclusters within the nanoscale gap (Fig. 2). Gold nanoclusters within these junctions not only electroluminesce, but also strongly fluoresce when excited at 532 nm, thereby enabling optically excited lifetimes of ~ 600 ps to be measured with pulsed laser excitation and time correlated single-photon counting detection (not shown). Ensemble Au electroluminescence lifetimes were measured to be slightly faster (~ 400 ps) through comparison with instrument response-limited Ag nanocluster emission. Optical excitation coaxes spectrally indistinguishable emission from more molecules than does electrical excitation (Fig. 2); however, as only a subset of Au nanoclusters have the proper electrical contacts to electroluminesce (EL), slight quenching of the emission likely produces the slightly shorter EL lifetime.

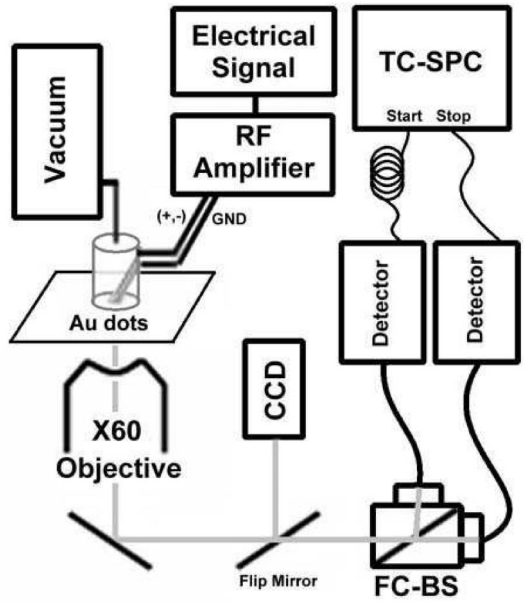

FIG. 1. Schematic of Hanbury Brown and Twiss interferometer for single molecule electroluminescence intensity correlation measurements. Electroluminescence from electrically contacted gold nanodots (10^{-5} torr) was projected onto a CCD camera through a high numerical aperture (NA = 1.45) oil-immersion 60x microscope objective. After further optical expansion of the image (1.6x), nanoclusters were positioned such that their spatially resolved emission was equally split, and aligned into two 100 μm multimode optical fibers coupled to single-photon sensitive avalanche photon diodes (APDs). Electrical pulses from the two detectors are inverted, delayed with respect to one another, and sent to the ''start'' and ''stop'' channels of a time-to-amplitude converter in a time correlated single-photon counting board (TC-SPC, Picoquant, TimeHarp 100). Start-stop photon pairs (coincidence counts) were recorded as a function of relative delay τ to produce an excellent approximation of the intensity correlation function, $g^{(2)}(\tau)$, at short times [29].

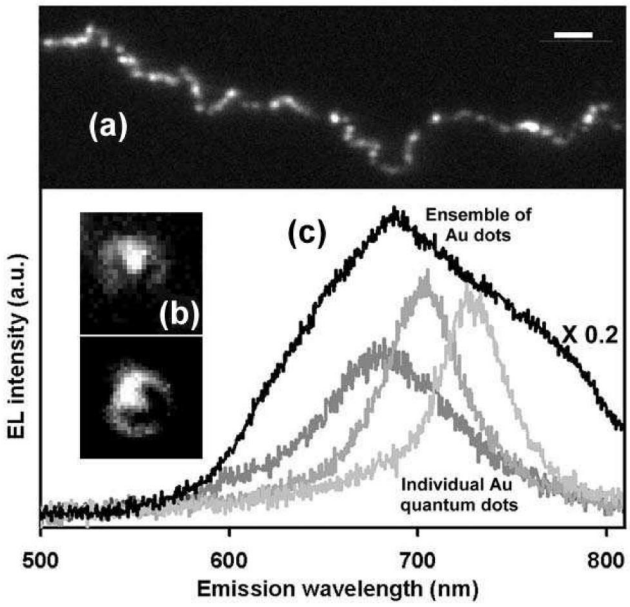

FIG. 2. Au nanodot electroluminescence. (a) Electroluminescence (EL) from a gold nanodot array within a nanoscale break junction under high frequency ac excitation (± 2.5 VAC, 220 MHz, scale bar: 5 μm). (b) Dipolar emission from individual dots [27]. (c) EL spectra of three typical single-gold quantum dots (gray traces) compared to that of an ensemble (black line). Although both homogeneously and inhomogeneously broadened, each single dot spectrum exhibits a much narrower linewidth than does the ensemble spectrum and they range in emission maximum from ~ 650 to ~ 750 nm, corresponding to sizes of 18–22 atoms [21]. All spectra were collected through a 300 mm imaging monochromator (acton) with a 150 l/mm grating.

Au nanoclusters within the nanoscale junctions are most conveniently excited with low voltage (5 V_{p-p}) ac frequencies corresponding to the junction transmission window at ~220 MHz. The junction acts as a bandpass filter that is properly impedance matched only at the frequency corresponding to the transmission maximum. These junctions operate effectively as series resistor-inductor-capacitor circuits, thereby enabling low power excitation at very high frequencies [25]. The junction transmission frequency is readily tuned through computer-controlled, dc-induced electromigration of the metal film. Individual Au nanoclusters are easily spatially isolated within the junction with continuous individual nanocluster emission remaining bright for several hours and junctions retaining many emissive nanoclusters for several days of operation. dc operation yields bright EL, but the high power necessary to overcome the high dc impedance rapidly restructures and destroys the junctions, precluding dc $g^{(2)}(\tau)$ measurements. Once obtained, ac-excited single nanocluster emission is equally split and aligned onto two 100 μm fiber-coupled avalanche photodiodes yielding detected electroluminescence count rates (>10 kHz) from individual features.

The spatial distribution of emissive nanoclusters within the junctions is asymmetric with more emitters being closer to the anode as defined by the dc fabrication process. Similar to our results involving silver [26], these gold junctions operate with overall asymmetry in emission and demonstrate weak light-emitting diode behavior due to preferential electron injection through the anode. The ensemble (multiparticle) $g^{(2)}(\tau)$ [Fig. 3(a)] shows sinusoidal oscillations at twice the ac drive frequency with alternating intensities. The intensity modulation at 220 MHz demonstrates that electroluminescence results from preferential injection through the anode (large peaks) but also occurs to a lesser extent through the cathode (manifested as smaller peaks shifted in phase by π). This interpretation is confirmed by the observation of light-emitting diode behavior with an overall preference for injection through the anode as measured by pulse polarity experiments. Further magnification of the electroluminescence image projected onto the fiber entrance enabled improved spatial discrimination and direct measurement of the intensity autocorrelation from individual nanocluster emission [Fig. 3(b)]. In this case, antibunched electroluminescence is clearly observed as a significantly reduced coincidence count rate at zero delay. Additionally, the peaks shifted by π (resulting from injection through the cathode) are also significantly smaller than in the ensemble measurement, indicating the asymmetric coupling of the individual nanocluster to each electrode. Although emission appears pulsed due to ac excitation and preferential injection through the semiconducting anode, it is important to point out that the behavior of $g^{(2)}(\tau)$ near zero time delay is more similar to that produced by dc or cw excitation [20] due to the fast emission lifetime relative to the ac excitation period and the relatively long detector response, as shown in the simulation in Fig. 3(b). Convolution of the single dot intensity autocorrelation with the finite instrument response has the overall experimental effect of attenuating the peak height at zero delay and giving an effectively constant offset to the overall function. Consequently, the high frequency (76 ps bins) intensity fluctuations are statistical noise as the time resolution is limited by the relatively long collective avalanche photodiode (APD) response of ~1.1 ns. This particular manifestation of the antibunching signature is well represented in simulations incorporating the

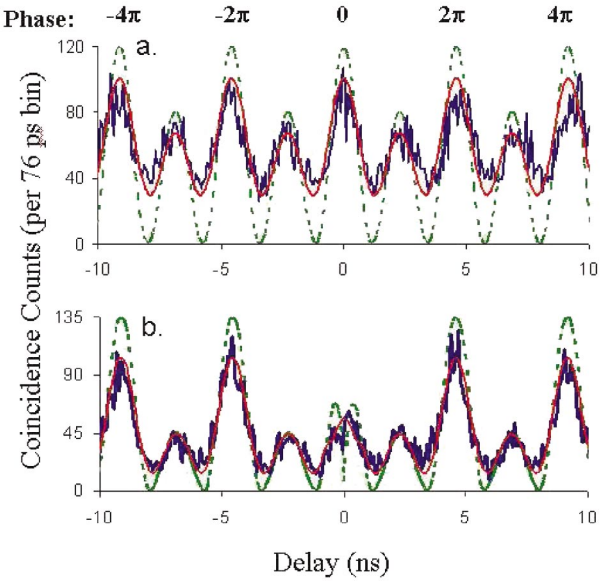

FIG. 3 (color). Measured (76 ps bins) and simulated second-order intensity correlation function $g^{(2)}(\tau)$ of gold electroluminescence driven at 220 MHz. (a) EL intensity autocorrelation from a group of many gold dots (blue) overplotted with an ideal simulation (green dotted line) and after convolution with the finite time response of our detectors (1.1 ns, red line), all showing the 220 MHz ac excitation frequency. Smaller peaks shifted in phase by π radians arise from electron injection through the cathode. (b) Antibunching in single Au nanocluster electroluminescence (blue), overplotted with an ideal simulation (green dotted line), and its convolution with the detector response (red line). The small probability for injection through the cathode is again evidenced by the smaller peaks shifted by π. As described by the simulations, the $g^{(2)}(0)$ peak in (b) is substantially diminished relative to peaks shifted by higher multiples of 2π. Much faster than the ac excitation period (~4.55 ns), and the time resolution of our two APDs (1.1 ns), the short emission lifetime (~400 ps) limits the observable contrast in $g^{(2)}(\tau)$ measurements but allows for high single-photon data rates. Although readily apparent after only ~100 s, the high contrast $g^{(2)}(\tau)$ at high repetition rates such as that in (b) is obtained in 25 min. Only low frequency intensity changes are statistically significant as the time resolution is much longer than the bin width used.

220 MHz excitation, 400 ps electroluminescence lifetime, and 80% (20%) injection efficiency through the anode (cathode) [Fig. 3(b)]. The experimentally observed degree of antibunching $[g^{(2)}(0)/g^{(2)}(2\pi) \sim 35\%]$ is consistent with simulations of an ideal single-photon source having essentially zero probability of simultaneous two-photon emission. However, we must acknowledge the possibility of a finite two-photon generation probability of ≤ 0.3 as a result of the obscuration of the true value of $g^{(2)}(0)$ that results solely from our detector time response.

The antibunched emission proves that Au nanoclusters behave as individual artificial atoms, and it opens new avenues for the study and application of small metal quantum dots in nanoscale quantum optoelectronics. The nanoclusters are small enough to have discrete, size-tunable emission at room temperature that can be harnessed to easily create arrays of electrically addressable single-photon sources. The high excitation rates (220 MHz) and short lifetimes produce high bit rates, at frequencies amenable to electro-optic polarization modulation, offering the ability to simultaneously drive an electro-optic modulator for in phase control of either polarization or intensity. Combined with the facile creation and utilization of room-temperature electrically excited single-photon source arrays, this offers the opportunity for synchronized modulation of both intensity and polarization for potential encryption schemes [3] using nonorthogonal polarization bases. In addition to their ease of fabrication, noble metal quantum dots are easily made to electroluminesce for several days of stable, room-temperature operation. These features could result in more easily transportable devices, making quantum cryptography much simpler to implement with true room-temperature nanoscale quantum optoelectronic elements.

R. M. D. gratefully acknowledges the Sloan, Dreyfus, and Vasser Woolley Foundations for their support of this work.

*To whom correspondence should be addressed. dickson@chemistry.gatech.edu

[1] C. H. Bennett and G. Brassard, in *Proceedings of the IEEE International Conference on Computers, Systems and Signal Processing* (IEEE, New York, 1984), p. 175.
[2] A. K. Ekert, Phys. Rev. Lett. **67**, 661 (1991).
[3] C. H. Bennett and D. P. DiVincenzo, Nature (London) **404**, 247 (2000).
[4] H. J. Carmichael, Phys. Rev. Lett. **55**, 2790 (1985).
[5] H. J. Kimble, M. Dagenais, and L. Mandel, Phys. Rev. Lett. **39**, 691 (1977).
[6] I. E. Lyublinskaya and R. Vyas, Phys. Rev. A **48**, 3966 (1993).
[7] M. Schubert *et al.*, Phys. Rev. Lett. **68**, 3016 (1992).
[8] J. McKeever *et al.*, Science **303**, 1992 (2004).
[9] B. Lounis and W. E. Moerner, Nature (London) **407**, 491 (2000).
[10] C. Brunel *et al.*, Phys. Rev. Lett. **83**, 2722 (1999).
[11] P. Kumar *et al.*, J. Am. Chem. Soc. **126**, 3376 (2004).
[12] T. Huser, M. Yan, and L. J. Rothberg, Proc. Natl. Acad. Sci. U.S.A. **97**, 11 187 (2000).
[13] C. Kurtsiefer *et al.*, Phys. Rev. Lett. **85**, 290 (2000).
[14] A. Beveratos *et al.*, Phys. Rev. A **64**, 061802 (2001).
[15] P. Michler *et al.*, Nature (London) **406**, 968 (2000).
[16] P. Michler *et al.*, Science **290**, 2282 (2000).
[17] E. Moreau *et al.*, Appl. Phys. Lett. **79**, 2865 (2001).
[18] J. A. Misewich *et al.*, Science **300**, 783 (2003).
[19] M. S. Gudiksen *et al.*, Nature (London) **415**, 617 (2003).
[20] Z. Yuan *et al.*, Science **295**, 102 (2002).
[21] J. Zheng, C. Zhang, and R. M. Dickson, Phys. Rev. Lett. **93**, 077402 (2004).
[22] R. Hanbury Brown and R. Q. Twiss, Nature (London) **178**, 1447 (1956).
[23] R. Loudon, *The Quantum Theory of Light* (Oxford University, New York, 2000).
[24] J. Zheng and R. M. Dickson, J. Am. Chem. Soc. **124**, 13 982 (2002).
[25] T.-H. Lee, J. I. Gonzalez, and R. M. Dickson, Proc. Natl. Acad. Sci. U.S.A. **99**, 10 272 (2002).
[26] T.-H. Lee and R. M. Dickson, J. Phys. Chem. B **107**, 7387 (2003).
[27] A. P. Bartko and R. M. Dickson, J. Phys. Chem. B **103**, 11 237 (1999).
[28] A. Zrenner, J. Chem. Phys. **112**, 7790 (2000).
[29] This measurement reflects the true intensity autocorrelation in the limit of short delays with respect to the inverse count rate. The 50 ns window in τ is well within the range afforded by our observed average count rate of $\sim$10 kHz.